Pergamon

PII: S0277-5387(97)00101-0

Polyhedron Vol. 16, No. 20, pp. 3663–3670, 1997

0277-5387/97 $17.00+0.00

Mechanism of electrophilic attack in (η^5-pentadienyl)Mn[$(Me_2PCH_2)_3CMe$] and (η^5-2,4-dimethylpentadienyl)Re$(PMe_2Ph)_3$

M. C. Milletti

Department of Chemistry, Eastern Michigan University, Ypsilanti, MI 48197, U.S.A.

(Received 9 January 1997; accepted 26 February 1997)

Abstract—Electrophilic attacks on both (η^5-pentadienyl)Mn[$(Me_2PCH_2)_3CMe$] and (η^5-2,4-dimethylpentadienyl)Re$(PMe_2Ph)_3$ are predicted to occur at the metal center, based on the results of *ab initio* molecular orbital calculations. Attack occurs at the open side of the pentadienyl ligand, although for both complexes the thermodynamic product exhibits a different configuration from that of the kinetic product. In the thermodynamic product of the manganese complex the proton resides in a semibridging position between the side of the pentadienyl ligand and the metal center. In the rhenium complex, the proton migrates to the back side of the pentadienyl ligand and bonds strongly with the metal center. © 1997 Elsevier Science Ltd

Many of the reactions involving organometallic transition metal complexes which have been used to model catalysis processes entail electrophilic or nucleophilic ligand attacks on the complexes. Despite the prevalence of these two types of reaction, there is still no proven method that can be used to reliably identify the site on the substrate molecule at which the attack will occur. While experimental data can often be used to characterize the thermodynamic product of the reaction, it is usually more difficult to pinpoint the immediate kinetic product of attack, especially if it differs from the thermodynamic product. It would be highly desirable, therefore, to develop a reliable correlation between structure and reactivity of organometallic complexes in these types of reactions, as has been so successfully done in organic chemistry [1].

The work of Klopman on chemical reactivity perhaps comes closest to outlining a general set of rules that can be used in predicting reactivity sites [2]. In his paper on chemical reactivity, Klopman categorizes electrophilic and nucleophilic attacks as being either charge- or frontier-controlled reactions. The above prediction is based on the difference in orbital energies between the incoming ligand and the substrate molecule. More specifically, if the energy difference between the frontier orbital of the substrate and that of the ligand is large, the reaction is said to be charge controlled; if it is negligible, the reaction will be frontier controlled. In the first case nucleophilic attack occurs at the position carrying the largest positive charge and electrophilic attack at the most negatively charged center. In the latter case a nucleophile attacks at the site where the LUMO of the substrate is localized and an electrophile will attack the area of the molecule where the HOMO is localized.

This work examines the reaction between H^+ and two related organometallic complexes, (η^5-pentadienyl)Mn[$(Me_2PCH_2)_3CMe$] and (η^5-2,4-dimethylpentadienyl)Re$(PMe_2Ph)_3$. In the manganese complex, the proton adds to the pentadienyl (pd) ligand and H is found to be agostic with the metal. On the other hand, an X-ray diffraction study finds the proton in the rhenium complex to be bound exclusively to the metal [3]. These two electrophilic attacks are investigated by analyzing the results of semiempirical [4] ad *ab initio* [5] molecular orbital calculations on the two related complexes. The reactions are analyzed in terms of mechanism of attack and whether the attacks are charge or orbital controlled.

COMPUTATIONAL PROCEDURE

Calculations were first carried out using complexes' X-ray structure coordinates with the Fenske–Hall semiempirical method [4] on a VAX mainframe com-

puter. Calculations on most complexes were also carried out with the GAUSSIAN 92 *ab initio* program [5], which allows for geometry optimization, at the Pittsburgh Supercomputing Center. Unless stated otherwise, results from the semiempirical calculations generally agreed with the *ab initio* ones.

In the Fenske–Hall calculations, atomic basis functions were employed; for phosphorus and carbon Clementi's double-ζ functions were used [6], except for 1s and 2s functions, which were curve-fit to single ζ by using the maximum overlap criterion [7]. For phosphorus, *d* basis set functions were employed. The hydrogen exponent was set to 1.16. The manganese and rhenium functions were taken from the results of Richardson *et al.* [8]. The 4*s* and 4*p* exponents for manganese were set to 2.0 and the 6*s* and 6*p* exponents for rhenium were set to 2.4, in order to avoid working with metal outer functions that are too diffuse, which often leads to meaningless results. GAUSSIAN 92 [5] *ab initio* calculations were also used to optimize the geometry of the manganese and rhenium protonated complexes and confirm the results obtained by the semiempirical calculations. For both manganese and rhenium complexes the LANL1MB basis set was used [9–11].

The geometric coordinates used for (η^5-pentadienyl)Mn[$(Me_2PCH_2)_3CMe$] [12], (η^5-2,4-dimethylpentadienyl)Re(PMe_2Ph)$_3$ [13], and [(η^5-2,4-dimethylpentadienyl)Re(H)(PMe_2Ph)$_3$]$^+$ [7] were taken from the X-ray structure data available in the literature. Calculations were also run on an idealized geometry for (η^5-pentadienyl)Mn[$(Me_2PCH_2)_3CMe$] and (η^5-2,4-dimethylpentadienyl)Re(PMe_2Ph)$_3$, in which the pd ring was centered above the metal. The geometry of the remaining intermediate compounds, for which there is no X-ray data, was optimized using the GAUSSIAN 92 program (*vide infra*) [14]. For simplicity of interpretation and greater ease in the calculations, the $(Me_2PCH_2)_3CMe$ and PMe_2Ph groups have been substituted with phosphine groups, while η^5-2,4-dimethyl-pentadienyl has been modeled by η^5-pentadienyl. The P–H distance was set to 1.420 Å.

RESULTS AND DISCUSSION

In order to determine whether the protonation reactions described above are charge or orbital controlled, it is necessary to know both the position and nature of the HOMO and the charge distribution in each complex. Predictions about the mechanism of attack can then be made on the basis of this information and compared with what is experimentally known about the protonated complexes.

Mn(pd)(PH_3)$_3$

GAUSSIAN 92 calculations were carried out on both the X-ray and the idealized structure of this complex. The idealized structure seems to be the more stable of the two, with both a lower total energy and a higher HOMO–LUMO gap (see Table 1). Fenske–Hall calculations on the idealized structure show similar results to the *ab initio* calculations: the HOMO of the molecule is delocalized between the metal and the pd ligand, especially the carbon atoms on the backbone of the open ring (see Fig. 1). The SHOMO* of the molecule is mostly metal-localized, with some contributions from the ring backbone carbons. The sites of largest negative charge in the molecule are on the pd ring, with the 'mouth' end carbons carrying a somewhat larger negative charge than the backbone carbons.

Table 1. Comparison of idealized and X-ray structures for Mn(pd)(PH_3)$_3$

	E_{RHF} (eV)	HOMO–LUMO gap (eV)
X-ray data	−6225	7.7
Idealized	−6238	8.4

Variable-temperature NMR spectra of (η^5-pentadienyl)Mn[$(Me_2PCH_2)_3CMe$] indicate that the proton attacks in an *endo* fashion either at the metal center, followed by migration at the semibridging site, or directly at the semibridging site [3]. The calculations reveal no orbital (HOMO or SHOMO) to support the second hypothesis. On the other hand, attack at the metal center is consistent with the large metal contribution to both the HOMO and the SHOMO. This, in turn, suggests that the reaction is orbital controlled.

In order to determine which orbitals are involved in the newly-formed metal-hydrogen bond, a calculation was carried out on the proposed protonated intermediate with the H^+ ion bonded directly to the metal. Starting with the idealized complex structure, the pro-

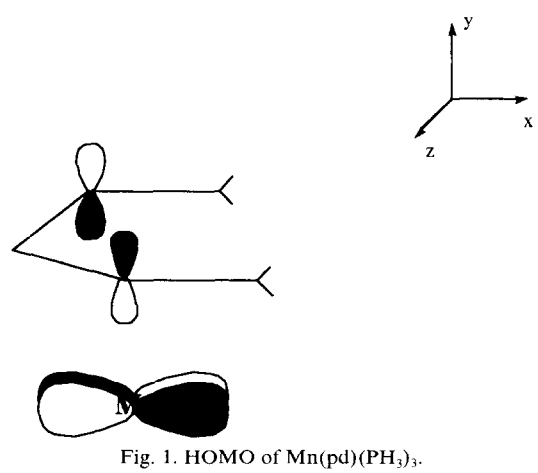

Fig. 1. HOMO of Mn(pd)(PH_3)$_3$.

* Second Highest Occupied Molecular Orbital.

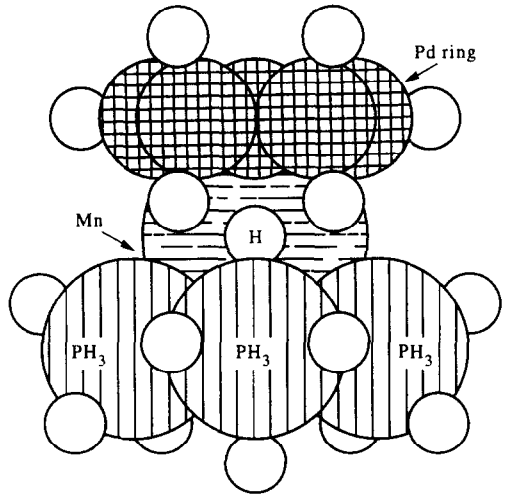

Fig. 2. Structure of the $[HMn(pd)(PH_3)_3]^+$ complex after initial attack of the proton at the metal center. The molecule is viewed from the open side of the pentadienyl ring. The position of the hydrogen atom has been optimized.

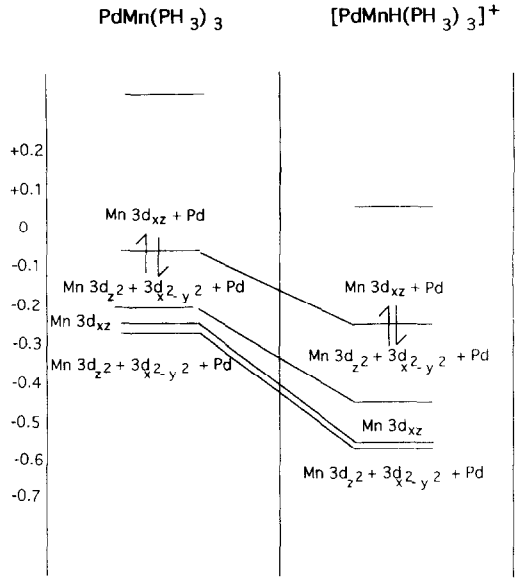

Fig. 4. Comparison of the molecular orbitals of the neutral manganese complex and the manganese cation protonated at the metal.

ton was initially placed in the cavity between the metal, the open side of the pd ligand and one of the phosphine ligands. The position of the H atom was then optimized, keeping the rest of the molecule rigid (see Fig. 2). When analyzing the molecular orbitals of this protonated complex, it is found that the orbital containing the Mn—H bond is the SHOMO, in which Mn valence d orbitals overlap with the H 1s orbital. This molecular orbital also receives minor contributions from the phosphine and pd ligands (see Fig. 3).

A comparison of the molecular orbitals of the neutral manganese complex and those of the intermediate protonated cation reveals that protonation of the complex at the metal center does not significantly change the order of the molecular orbitals (see Fig. 4). Apart from the energy lowering of all orbitals in the cation because of the overall positive charge, the order of the valence molecular orbitals remains the same. Both the HOMO and the SHOMO of the complexes are Mn–pd bonding in nature and it is the SHOMO that offers the most stable interaction with the incoming proton.

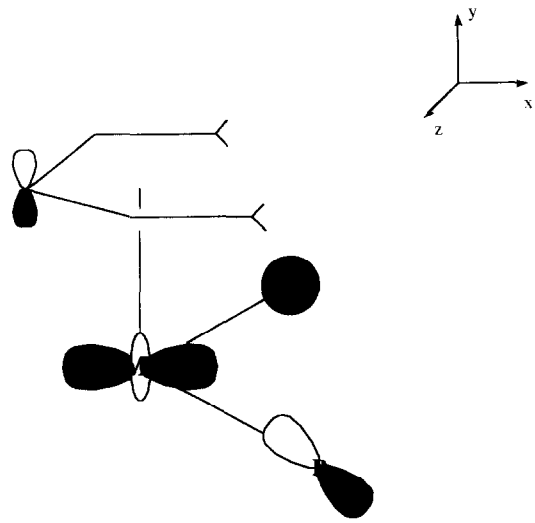

Fig. 3. SHOMO of the $[HMn(pd)(PH_3)_3]^+$ complex shown in Fig. 2. This orbital houses the bulk of the Mn—H bond.

The nature of the thermodynamic protonated product was examined next. From experimental evidence, the proton is thought to be in a semibridging position between the metal and the pd ring, but no other experimental structural information is available. Therefore, the position of the agostic proton was optimized with the GAUSSIAN 92 program. This time the positions of the four hydrogens bonded to the pd mouth carbons, as well as that of the semibridging hydrogen, were left flexible during the geometry optimization. The most stable position for the semibridging proton was found to be equidistant from one of the phosphine ligands, one of the pd mouth carbons, and one of the pd backbone carbons (approximately 1.8 Å from each of these centers). The agostic hydrogen is also closest to the Mn center and one of the hydrogens bonded to the mouth carbon (1.4 and 1.5 Å, respectively). Surprisingly, in the thermodynamic product the agostic hydrogen has shifted out of the cavity formed by the open side of the pd ring, the metal center, and one of the phosphine ligands, and is now bridging on one of the backbone sides of the pd ligand (see Fig. 5).

An examination of the molecular orbitals reveals that the agostic hydrogen contributes most to the HOMO and SHOMO of the molecule. In the HOMO, the agostic hydrogen is bonded to the metal and the backbone carbon, while it is out of phase with the

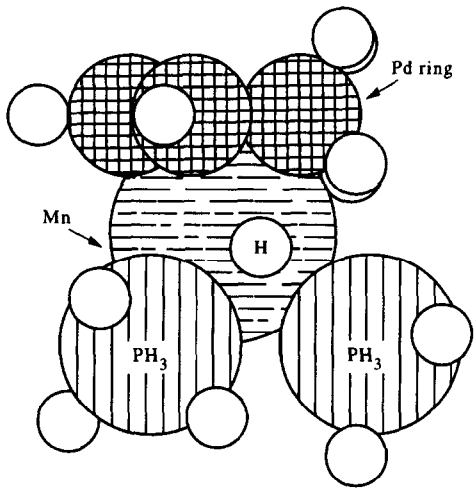

Fig. 5. Structure of the $[Mn(H)(pd)(PH_3)_3]^+$ complex. The molecule is viewed from the side of the pentadienyl ring. The positions of the semibridging hydrogen and the four hydrogens at the 'mouth' of the Pd ligand have been optimized.

Table 2. Mulliken overlap populations for $[Mn(H)(pd)(PH_3)_3]^+$

	H (semibridging)
Mn $3d_{z^2}$	0.0884
Mn $3d_{xz}$	0.0643
Mn s	0.0305
Mn p_y	0.0398
C $2p_y$[a]	0.0455
H $1s$[b]	−0.0380
P $3s$	−0.0261
C $2s$[c]	−0.0226

[a] pd backbone carbon.
[b] bonded to pd mouth carbon.
[c] pd mouth carbon.

hydrogen of the mouth carbon. In the SHOMO, the semibridging hydrogen is bonding again with Mn, but it is out of phase with the phosphine P. These trends are again evident in the Mulliken population analysis [15], which shows the strongest overlap populations with the metal and the backbone carbon orbitals and out of phase overlap with the mouth C and its H and the phosphine P (see Table 2).

The shift in the position of the semibridging hydrogen from inside the cavity created by the pd mouth, the metal, and one of the phosphines (Fig. 2) to under the backbone side of the pd ligand (Fig. 5) is due to the increased stability of the proton in the latter position. This is evidenced by the increase in the amount of overlap population between the semibridging hydrogen and neighboring centers, the larger HOMO/LUMO gap, and lower total energy for the complex in Fig. 5 (see Table 3).

In conclusion, electrophilic attack on the Mn(pd)$(PH_3)_3$ complex is orbital controlled. Since the HOMO and the SHOMO of the complex receive large contributions from the metal center, attack occurs at the metal. The newly-formed metal-hydrogen bond is evident mainly in the SHOMO of the protonation's kinetic product. In the thermodynamic product, the hydrogen moves to a position in which it bridges between one of the backbone sides of the pd ligand and the metal center, forming the stronger bond with the metal.

$Re(pd)(PH_3)_3$

An *ab initio* molecular orbital calculation was performed also on the rhenium analog of the manganese complex. The geometry of the rhenium complex was idealized to *Cs* symmetry, so that the results could be compared to those for the manganese complex. Results of the calculation show that the valence molecular orbitals consist of pd–Re interactions, which are out-of-phase for both the HOMO and the LUMO. In particular, the HOMO has equal contributions from the metal and the ligand, with the backbone carbons on the ligand contributing more than the mouth carbons. On the other hand, the SHOMO involves a bonding interaction between the metal and the unique backbone carbon of the pd ring. Diagrams for both molecular orbitals are shown in Fig. 6; the HOMO–SHOMO gap is approximately 3 eV. In terms of the charge distribution in the molecule, the sites of largest negative charge are the pd mouth carbons (-0.20 e$^-$ each) and the P atom of the phosphine ligand located underneath the 'mouth' of the pd ligand (-0.22 e$^-$).

Based on spectroscopic evidence, Bleeke and coworkers favor a mechanism of reaction that involves initial kinetic attack at the rhenium center from the open (mouth) side of the pd ligand, followed by rapid exchange of the metal-bound hydrogen atom with the

Table 3. Comparison of kinetic and thermodynamic products of protonation of $Mn(pd)(PH_3)_3$

	Sum of overlap pops.	HOMO–LUMO gap (eV)	E_{RHF} (eV)
$[Mn(H)(pd)(PH_3)_3]^+$ kinetic product H^+ under pd mouth	0.0551	8.9	−6229
$[Mn(H)(pd)(PH_3)_3]^+$ thermodynamic product H^+ under pd backbone	0.1695	11.9	−6240

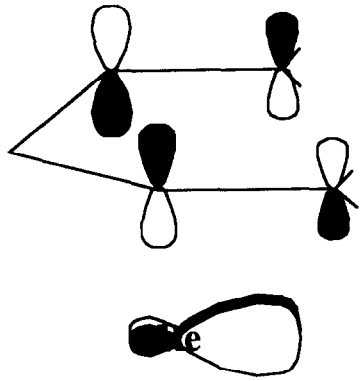

a.

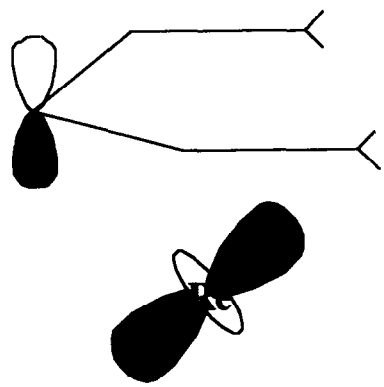

b.

Fig. 6. (a). HOMO and (b). SHOMO of $Re(pd)(PH_3)_3$.

other hydrogens on the mouth carbons. Subsequently, the kinetic product converts to the thermodynamic product, where the metal-bound hydrogen resides under the backbone of the pd ligand [3]. Considering the results of the molecular orbital calculation discussed above, the proposed mechanism suggests that the reaction is again orbital controlled: if attack is to occur at the metal, it must proceed through the HOMO and/or SHOMO of the complex, both of which have large metal contributions. In addition, both orbitals show a larger amount of electron density at the metal on the side of the 'mouth' of the pd ligand, suggesting that as the preferred side for the incoming proton to approach the metal. While the SHOMO shows a lone-pair-like lobe of hybridized *d* orbitals on the metal which would make it a prime candidate, the HOMO includes electron density at the mouth carbons of the pd ligand, which would facilitate exchange of the proton between the metal and the mouth carbons, as suggested by the spectroscopic data.

Similarly to what was done for the manganese complex, a calculation was carried out on the proposed kinetic product, where the proton is bound to the metal under the open side of the pd ligand. As with the manganese complex, the position of the hydrogen was optimized, leaving the idealized geometry of the remainder of the complex unchanged. The optimized position for the hydrogen was found to be at 1.6 Å from the metal center and at an angle of 80° with the center of the pd ring.

An analysis of the molecular orbitals for the kinetic product reveals that the SHOMO of the neutral complex is the most likely site of attack; in the kinetic protonation product, the hydrogen 1*s* orbital contributes to the two molecular orbitals below the HOMO and to two other molecular orbitals at lower energies. In these orbitals, in-phase overlap is found between the hydrogen 1s orbital and the metal center, the two hydrogens on the pd ring closest to it, and the phosphine P atom below the open side of the pd ring. The effect of protonation on the overall molecular orbital diagram is simply to lower the energy of all valence molecular orbitals (see Fig. 7); there is still a one-to-one correspondence between the neutral complexes molecular orbitals and those of the protonation kinetic product.

As was done for the manganese complex, the thermodynamic product of the protonation of the rhenium compound was examined next. Following the structure suggested by the X-ray analysis, the proton was initially bonded to the metal under the backbone side of the pd ligand. The position of the proton and all three phosphine ligands was then optimized. The optimized Re—H bond length was found to be 1.7 Å and the angle between the proton, the metal, and the center of the pd ring was 127° (see Fig. 8). Notice that the two phosphine ligands closest to the back of the pd ligand have shifted substantially to accommodate the Re—H bond.

A comparison of the molecular orbital diagram for the kinetic and thermodynamic products of electrophilic attack on $pdRe(PH_3)_3$ shows the greater stability of the thermodynamic product (Fig. 9). Notice also that in the thermodynamic product the Re—H bond is almost entirely found in a single molecular orbital, where the metal orbitals are strongly overlapping with the H 1s orbital. In the kinetic product, the Re—H interaction is spread out over at least two valence molecular orbitals. Both of these orbitals are at a higher energy than the corresponding orbital in the thermodynamic product and they involve more than just the metal–hydrogen interaction. In summary, the configuration adopted by the hydrogen atom in the thermodynamic product leads to a stron-

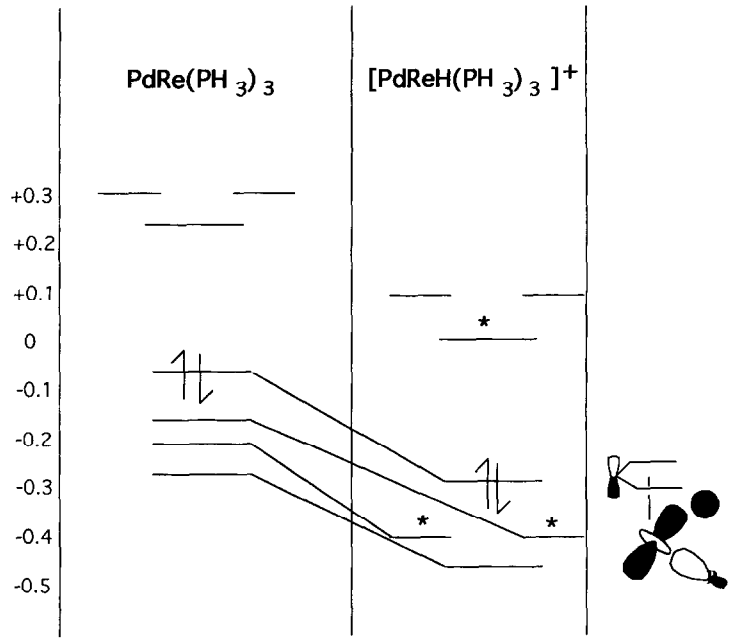

Fig. 7. Comparison of the molecular orbitals of the neutral rhenium complex and those of the protonation kinetic product. Significant contributions from the H^+ 1*s* orbital appear in the starred molecular orbitals.

Table 4. Comparison of kinetic and thermodynamic products of protonation of $Re(pd)(PH_3)_3$

	Total Re—H overlap pop.	HOMO–LUMO gap (eV)	E_{RHF} (eV)
$[Re(H)(pd)(PH_3)_3]^+$ kinetic product H^+ under pd mouth	0.1921	7.2	−6122
$[Re(H)(pd)(PH_3)_3]^+$ thermodynamic product H^+ under pd backbone	0.3770	9.8	−6132

ger Re—H bond and more stable complex, as evidenced by the data in Table 4.

In conclusion electrophilic attack on $Re(pd)(PH_3)_3$ is also orbital controlled. Since the HOMO and SHOMO of the complex have large Re contributions, attack can occur at the metal center, followed by migration of the H atom to the backside of the complex, where the Re—H bonding interaction is maximized.

CONCLUSIONS

The results of *ab initio* molecular orbital calculations and geometry optimizations shows that electrophilic attack on complexes of the type (η^5-pentadienyl)$M(PR_3)_3$ (M = Mn, Re) are orbital controlled. Since the occupied valence orbitals of these compounds contain large metal contributions, protonation initially occurs at the metal center. In the kinetic products the proton is bound to the metal in the cavity created by the 'mouth' of the pentadienyl ligand and one of the phosphine ligands. Subsequently, the hydrogen atom migrates to a position where it is able to maximize its bonding interaction with neighboring atoms. For the manganese complex, this position is under one of the sides of the pentadienyl ligand, where the proton can interact with two of the pd carbons and the metal simultaneously. In the rhenium complex, the hydrogen atom migrates to the backside of the complex, where it overlaps mostly with metal orbitals.

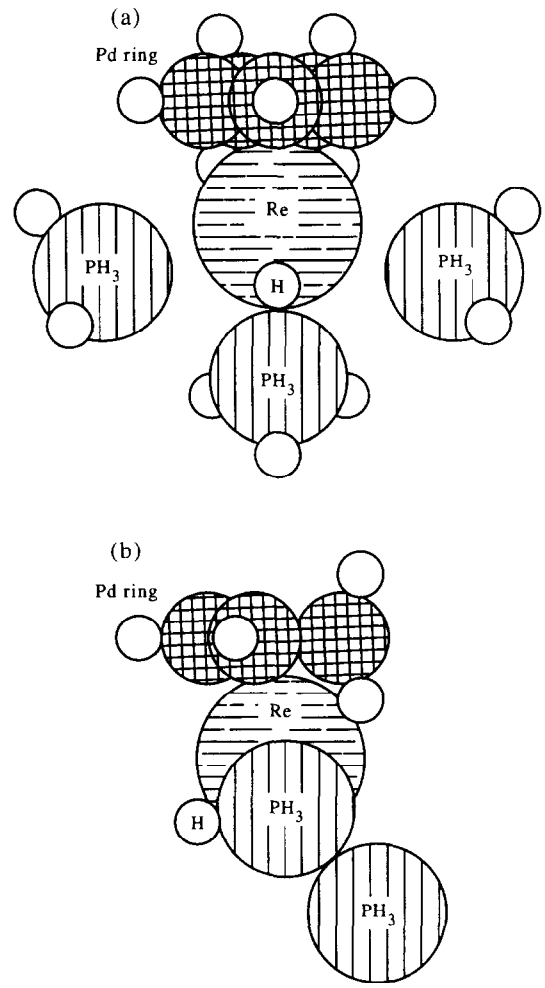

Fig. 8. Structure of the $[HRe(pd)(PH_3)_3]^+$ complex (thermodynamic product). The molecule is viewed (a) from the back and (b) from the side of the pentadienyl ring. The positions of the hydrogen bound to the metal and the three phosphine ligands have been optimized.

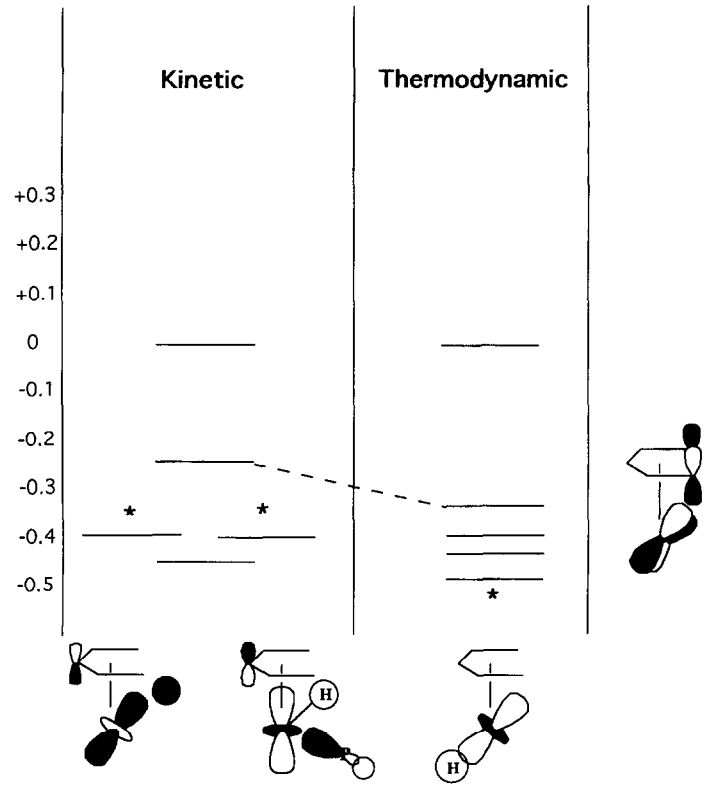

Fig. 9. Comparison of the molecular orbitals of the kinetic and thermodynamic products of electrophilic attack on $Re(pd)(PH_3)_3$. Starred orbitals have predominant Re—H bonding character. A representation of the major contributions to the starred molecular orbitals is shown below each of the orbitals. The sketch to the side of the diagram represents the HOMO of both complexes.

REFERENCES

1. Hudson, R. F., in *Chemical Reactivity and Reaction Paths*, G. Klopman, Ed., Wiley, New York, 1974, Chapter 5.
2. Klopman, G. *J. Am. Chem. Soc.* 1968, **90,** 223.
3. Bleeke, J. R., Kotyk, J. J., Moore, D. A. and Rauscher, D. J., *J. Am. Chem. Soc.* 1987, **109,** 417.
4. Hall, M. B. and Fenske, R. F., *Inorg. Chem.* 1972, **11,** 768.
5. Gaussian 92, Revision E.1, Frisch, M. J., Trucks, G. W., Head-Gordon, M., Gill, P. M. W., Wong, M. W., Foresman, J. B., Johnson, B. G., Schlegel, H. B., Robb, M. A., Replogle, E. S., Gomperts, R., Andres, J. L., Raghavachari, K., Binkley, J. S., Gonzalez, C., Martin, R. L., Fox, D. J., Defrees, D. J., Baker, J., Stewart, J. J. P. and Pople, J. A. Gaussian, Inc., Pittsburgh PA, 1992.
6. Clementi, E., *J. Chem. Phys.* 1964, **40,** 1944.
7. Radtke, D. D., Ph.D. Thesis, University of Wisconsin, Madison, WI (1966).
8. Richardson, J. W., Niewpoort, W. C., Powell, R. R. and Edgell, W. F., *J. Chem. Phys.* 1962, **36,** 1057.
9. Hay, P. J. and Wadt, W. R., *J. Chem. Phys.* 1985, **82,** 270.
10. Wadt, W. R. and Hay, P. J., *J. Chem. Phys.* 1985, **82,** 284.
11. Hay, P. J. and Wadt, W. R., *J. Chem. Phys.* 1985, **82,** 299.
12. Bleeke, J. R., Stanley, G. G. and Kotyk, J. J., *Organometallics* 1986, **5,** 1642.
13. Bleeke, J. R., Moore, D. A., *Inorg. Chem.* 1986, **25,** 3522.
14. Schlegel, H. B., *J. Comp. Chem.* 1982, **3,** 214.